The Second TSME International Conference on Mechanical Engineering
19-21 October, 2011, Krabi

3D Finite Element Analysis of Configurational Forces in Surface Coating

Ek-u THAMMAKORNBUNJUT[1], and Shoji IMATANI[1,*]

[1] Department of Energy Conversion Science, Kyoto University, Sakyo-ku, Kyoto, Japan, 606-8501

*Corresponding Author: imatani@energy.kyoto-u.ac.jp, Tel/Fax +81 (0) 75 753 4915

Abstract

This paper aims to study failures at the interface of a surface coating with perfect bonding subjected to thermal loads. The finite element method with elastoplastic constitutive relations is employed in order to simulate the interfacial characteristics of a film/substrate system. In addition, the configurational (or inhomogeneity) force based on the concepts of Eshelby's energy momentum tensor is also introduced and numerically evaluated by the finite elements. In context of the variation and magnitude of the inhomogeneity forces at the interface, effects of small interfacial roughness, crystal morphology, and temperature gradient are examined and discussed as a cause to generate a driving force of delamination.

Keywords*:* Debonding, Inhomogeneity force, Thermal stress, Finite element analysis.

1. Introduction

For some structural parts which are coated with different materials in order to improve their resistances to corrosion and/or high thermal environments, an interfacial debonding is one of the important problems to be considered. Mismatch of the coefficients of thermal expansion and residual stresses are the primary causes of this failure. The problems are generally modeled as film/substrate systems subjected to thermal loading and the film has higher coefficient of thermal expansion than the substrate. Therefore the biaxially compressive stresses will be induced in the film and cause the film to debond and buckle. These models have been studied based on fracture mechanics or combined with buckling (see, for example, [1-7]) which an initial crack or delamination must be assumed at the interface. Interfacial roughness was also considered by Hutchinson et al [5] and Liu et al [7]. Theoretical and numerical analyses were used and yielded very good results for some parameters such as stress intensity factors, energy release rates, and stress distributions. These solutions are related to the critical load and geometry of the models which affect to the propagation of the crack or delamination.

The researches above have been focused on geometry of the model such as thicknesses of the film and the substrate, shapes and dimensions of the debonding part, and

surface roughness at the interface. An effect of temperature gradient was included in some studies [1, 7]. However, these studies may produce only the solutions or charts which will be guidelines for design processes or be suggestions for properly working conditions of coated structures. The questions such as "What are the parameters which act like a driving force of the debonding in microscopic scale?" and "What will happen if the initial delamination is not assumed?" have been remaining. So, in the present study, we model the film/substrate system in a quasi-crystal scale in order to study the microscopic behavior of surface coating. The effects of crystal morphology, interfacial roughness, and temperature gradient are considered and the healthy bonding is also assumed. The problem is firstly modeled by the finite element method and then analyzed in the framework of the concept of configurational mechanics [8-10] or mechanics in material space [11] which is based on the energy-momentum tensor, introduced by Eshelby in 1951 [12].

A three-dimensional finite element method with thermo-elastoplastic constitutive model is carried out in order to simulate the thermomechanical response of a coated layer. An eight-node brick element with stabilized technique [13] is employed and formulated to a simple cubic block by using the voxel mesh generation. Material anisotropy with temperature dependence of the film and the substrate is also accounted. The anisotropic vectors $\boldsymbol{m}^{(1)}$, $\boldsymbol{m}^{(2)}$, and $\boldsymbol{m}^{(3)}$ of each crystal are mutually orthogonal in the initial state and evolve during the deformation. We use kinematic hardening rule in plastic deformation. Material model and the configurational force concepts will be briefly described in the following section. Then the analytical scheme and numerical results will be discussed.

2. Material Model and Configurational Forces

The material in this study is a nickel film deposited to a martensitic stainless steel by an electrochemical process. It is designed for a stamping tool of CD and/or DVD at high temperature. The coated structure is subjected to the temperature that slowly increased from 0°C to 500°C. In laboratory, the test pieces are prepared and, after tests, the delamination can be observed and verified by the indentation testing [14].

2.1 Models of film/substrate system

The test specimen is a beam with coated layers on top and bottom sides as shown in Fig. 1. Due to its symmetry, a small cubic element at an upper half of a symmetric plane is selected as a model of the film/substrate system. Each crystal is drawn in distinct color and the film and the substrate are separately displayed but they are connected in the real analysis. The thermal expansion coefficients are set to 1.0×10^{-5} $1/^{\circ}$C, and 1.3×10^{-5} $1/^{\circ}$C for the steel and nickel layer, respectively. It is assumed that the temperature dependence of the yield stress and Young's modulus are set to be decreasing functions linear on the temperature.

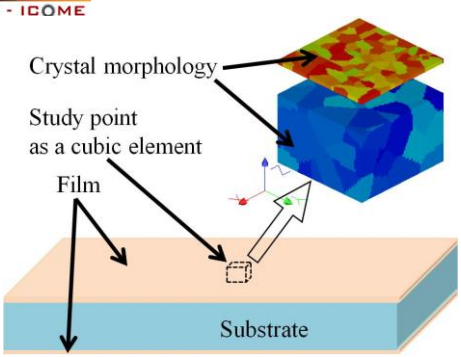

Fig. 1 A cubic crystal model of a coated body.

2.2 Constitutive Relations

In the following, we briefly summarize the constitutive model for anisotropic thermo-elasto-plastic materials with temperature dependence based on our recent work [14].

The total strain rate can generally be decomposed into the elastic $\dot{\varepsilon}_{ij}^{e}$, plastic $\dot{\varepsilon}_{ij}^{p}$, and thermal strain rates $\dot{\varepsilon}_{ij}^{t}$ as

$$\dot{\varepsilon}_{ij} = \dot{\varepsilon}_{ij}^{e} + \dot{\varepsilon}_{ij}^{p} + \dot{\varepsilon}_{ij}^{t} \quad (1)$$

The elastic component follows the Hooke's law of linear elasticity with cubic anisotropy and temperature dependence. By applying Spencer's works [15] to the fourth order elasticity tensor and limit our reduction to the simple cubic anisotropy, the elasticity tensor takes the form

$$E_{ijkl} = \mu\left(\delta_{ik}\delta_{jl} + \delta_{il}\delta_{jk}\right) + \lambda\delta_{ij}\delta_{kl} + a_e\left(L_{ij}L_{kl} + M_{ij}M_{kl} + N_{ij}N_{kl}\right)\theta(T) \quad (2)$$

L_{ij}, M_{ij}, and N_{ij} are structural tensors and are defined by

$$L_{ij} = m_i^{(1)}m_j^{(1)} - \frac{1}{3}\delta_{ij}$$
$$M_{ij} = m_i^{(2)}m_j^{(2)} - \frac{1}{3}\delta_{ij} \quad (3)$$
$$N_{ij} = m_i^{(3)}m_j^{(3)} - \frac{1}{3}\delta_{ij}$$

where the anisotropic vector $m_i^{(k)}$ (k = 1, 2, and 3) are mutually orthogonal and the intensity of the preferred orientation is identical. There are four material parameters which are Lame's constant μ and λ, elastic anisotropy a_e and the temperature dependent term $\theta(T)$, for the elastic part.

For plastic part, a quadratic yield function within a special case of Hill's formula is employed for the yield criterion, accounting for the kinematic back stress [14, 16]. The yield function is expressible in

$$F = \frac{1}{2}A_{ijkl}\left(\sigma_{ij} - \beta_{ij}\right)\left(\sigma_{kl} - \beta_{kl}\right) - \frac{1}{3}\sigma_Y^2 = 0 \quad (4)$$

The fourth order tensor takes a similar form to elasticity tensor as

$$A_{ijkl} = \frac{1}{2}\left(\delta_{ik}\delta_{jl} + \delta_{il}\delta_{jk}\right) - \frac{1}{3}\delta_{ij}\delta_{kl} + a_p\left(L_{ij}L_{kl} + M_{ij}M_{kl} + N_{ij}N_{kl}\right) \quad (5)$$

We use the Ziegler law for the evolution of the back stress and assume that stress-strain relation follows the power law as

$$\bar{\sigma} = c(b + \bar{\varepsilon}^p)^n \quad (6)$$

where $\bar{\sigma}$ and $\bar{\varepsilon}^p$ are the equivalent stress and strain, respectively. The parameter c depends on temperature so that the initial yield stress $\sigma_Y = cb^n$ is also dependent on temperature. We have four material parameters a_p, c, b, and n for plasticity where a_p stands for plastic anisotropy.

For the thermal part, the thermal expansion is still isotropic for cubic anisotropy and can be written as

$$\dot{\varepsilon}_{ij} = \alpha\dot{T}\delta_{ij} \quad (7)$$

where α and T are an average thermal expansion and temperature, respectively, and δ_{ij} is the Kronecker's delta.

The finite element model is implemented based on the updated Lagrangian (UL) formulation. A simple cubic block with crystal morphology is formulated by Voronoi tessellation

and voxel mesh generation. The film/substrate model is heated up to a designated temperature by prescribing the displacement in accordance with every step of an incremental temperature.

2.3 Configurational Forces

While the Newtonian concept of a force concerns with the motion and/or deformation of an object in the space (which will be called the physical space) of our surroundings, the Eshelbian force is an energy change of a system due to defects or inhomogeneities which alter the configuration of that system [11]. In his paper [12], Eshelby introduced the concept of the energy momentum tensor as a rate of change of the energy density with respect to the position of the defect (or singularity). This was done in a space which is later called material space [8, 11]. We mention here that the configurational forces [9, 11, 17, 18], the material forces [11, 19, 20], and the inhomogeneity forces [8], are identical and are based on the same concept of force. In the following paragraphs we briefly outline the derivation of the configurational force and apply it to this problem.

For finite deformation theory, the static equilibrium equation in the physical space can be expressed as

$$\frac{\partial P_{Ki}}{\partial X_K} + f_i = 0 \qquad (8)$$

where $P_{Ki} = \partial W / \partial F_{iK}$ is the first Piola-Kirchhoff stress tensor, f_i is a body force, X_K denotes coordinates with respect to the reference configuration and W stands for a strain energy density which is a function of the deformation gradient F_{iK}. For inhomogeneous materials, the strain energy density will depend on the deformation gradient and also the position itself. Therefore it should be expressed as $W(F_{iK}, X_K)$. In absent of the body force $(f_i = 0)$, applying the virtual work principle to Eq. (8) with $\delta x_i = -F_{iL}\delta X_L$, thus

$$\int \delta x_i \frac{\partial P_{Ki}}{\partial X_K} dV = -\int F_{iL}\delta X_L \frac{\partial P_{Ki}}{\partial X_K} dV = 0 \qquad (9)$$

and after manipulating several integration by part, we obtain

$$\int \delta X_L \left(\frac{\partial b_{KL}}{\partial X_K} + f_L^{inh} \right) dV = 0 \qquad (10)$$

where $b_{KL} = W\delta_{KL} - P_{Ki}F_{iL}$ is the Eshelby stress tensor or energy momentum tensor, and δ_{KL} is the Kronecker delta function. In addition, a kind of body force arising due to a nonvanishing configurational (or inhomogeneity) force in material space is given by

$$f_L^{inh} = -\left.\frac{\partial W}{\partial X_L}\right|_{expl} \qquad (11)$$

Here the subscript $expl$ denotes the explicit derivative of W with respect to the position X in the reference configuration.

From Eq. (10), the local form of the equilibrium equations in the material space can be written as

$$\frac{\partial b_{KL}}{\partial X_K} + f_L^{inh} = 0 \qquad (12)$$

which has an identical form as Eq. (8).

To obtain the inhomogeneity force, integrate Eq. (12) over a small volume V_0 and adopting the divergence theorem as

$$\left.\frac{\partial W}{\partial X_L}\right|_{expl} \cdot V_0 \cong -\int f_L^{inh} dV = \int b_{KL} N_K dS = \int (W\delta_{KL} - P_{Ki}F_{iL}) N_K dS \qquad (13)$$

Applying the Eq. (13) to non-isothermal processes, when subtracting the thermal expansion component from the total deformation,

i.e. $\widetilde{\boldsymbol{F}}^{ep} = \boldsymbol{F}\boldsymbol{F}^{\theta-1}$, we get the inhomogeneity force as

$$G_L^{inh} = \int \tilde{b}_{KL}\tilde{N}_K dS = \int (\tilde{W}\delta_{KL} - \tilde{P}_{Ki}\tilde{F}_{iL})\tilde{N}_K dS \quad (14)$$

at the intermediate configuration. $\tilde{W}$ and $\tilde{P}_{Ki}$ in Eq. (14) are also evaluated as the net elastic-plastic strain energy density and the first Piola-Kirchhoff stress tensor at the intermediate configuration. It should be noted here that $G_L^{inh} = 0$ if the body is homogeneous and no other material and geometric discontinuities such as bimaterials and a crack, respectively.

In case of small deformation, Eq. (14) can be rewritten as

$$G_l^{inh} = \int (W\delta_{kl} - \sigma_{ki}\frac{\partial u_i}{\partial x_l})n_k ds \quad (15)$$

where σ_{ki} is the Cauchy stress, x_l stands for the coordinates with respect to the current configuration, and u_i are the displacements. It can be pointed out that, one of the components of G_l^{inh}, i.e. $l = 1$, in Eq. (15) can be expressed as

$$G_1^{inh} = J = \int (W dx_2 - \sigma_{ki}\frac{\partial u_i}{\partial x_1}n_k ds) \quad (16)$$

which is the Rice's J-integral [25] in two dimensions. In comparison, the inhomogeneity force is proportional to the square of the macroscopic average stress as the J-integral which is proportional to the square of the stress intensity factor. In addition, the planar component of the inhomogeneity force can be defined as $\sqrt{G_x^{inh\,2} + G_y^{inh\,2}}/area$ which would be an important quantity in order to examine other parameters which may affect to the driving force of the debonding at the interface of bimaterial structures.

3. Analytical Scheme

3.1 Model Setting

Two main analytical models A and B with different sizes are generated as shown in Fig. 2. The model A has a substrate block size of 264×264×214 μm with 66×66×30 cubic elements whereas the coated layer has a size of 264×264×10 μm with 66×66×5 elements. At this level the effect of crystal morphology may appear. The color contour in each crystal implies distinct crystals with the same set of orientation $\boldsymbol{m}^{(i)}$. Therefore, the finite element model reflects a real material but sufficiently simplified. This model is used to examine the effect of interfacial roughness and crystal morphology. For the model B, a size of the substrate is five times larger than the model A's which is 1.32×1.32×1.07 mm while a size of the film is ten times thicker, i.e. 1.32×1.32×0.10 mm. At this level the microscopic effect for the layer may be neglected. So we can assume that the film material is isotropic while the crystal-like structure still remains for the substrate with the average size of about 80 μm. This model is used to evaluate the effect of temperature gradient in thickness direction. A small roughness is still introduced at the interface. The material is heated up from 0°C to 550°C which induces the compressive stresses into the film. However, elastic deformation is mostly observed while plastic yielding will be appeared around 500°C.

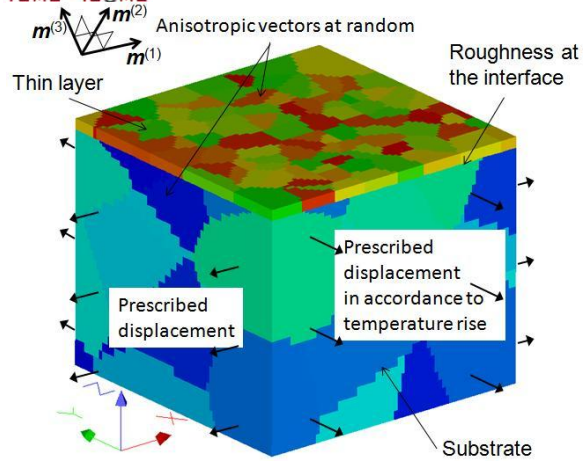

Fig. 2 Analytical model of coated materials.

3.2 Scenario of the Analysis

To evaluate the variation of the inhomogeneity forces in terms of interfacial roughness and crystal morphology, we divided the model A into three sub-models as follows:

(A1) Absolutely flat plane at the interface, which only crystal morphology will affect the inhomogeneity forces,

(A2) Random interfacial roughness within 0.2 μm height at every node, and

(A3) Random interfacial roughness within 0.6 μm height in order to emphasize the roughness effect.

In this analysis, the temperature is assumed to be uniform for the whole body.

In our problem, coated layers are used in high temperature conditions. So, we examine the effects of the temperature gradient on another model B. The temperature distribution is uniform in any planar direction while it is a linear function in the thickness direction. Three sub-models B are:

(B1) No temperature gradient, i.e. the temperature is uniformly heated up for whole body,

(B2) Reduce of 10°C in the total thickness of 1.17 mm from top to bottom surface,

(B3) Reduce 20°C in the total thickness.

Note that we set a small difference in temperature only 1 and 2°C within the thickness of the layer to reduce the effect of bending to the variation of the inhomogeneity forces. The interfacial roughness within 1 μm is also introduced in order to proportional to the case A2, accounting for the difference of the sizes between two models.

4. Equivalent Plastic Strain

From the finite element method, Fig. 3 shows the equivalent plastic strain distribution of the film on the substrate at 500°C while most of the substrate part is still in an elastic range due to their largely different dimension in the thickness direction. A wavy pattern with relatively long space frequency can be found, which implies that not only the crystal morphology of film but also the crystal of substrate affects the deformation characteristics of the film layer. However, the effect of surface roughness slightly develops in the analysis because of the constraint by the substrate. However, we cannot obtain any more details that which parameters have more influence to the driving force of the delamination from this simulated result.

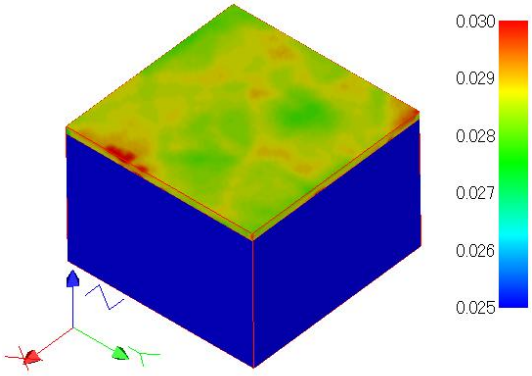

Fig. 3 Accumulation of equivalent plastic strain in the film.

5. Evolution of Inhomogeneity Forces

Fig. 4 shows the variation of the inhomogeneity force when temperature rises from 400°C to 550°C. Both normal and planar components develop when the temperature increases, and the planar component shows much smaller in the case of A1 while two decimal orders larger in the case of A3. The scatter also develops and so the roughness at the interface enhances the evolution of the inhomogeneity forces.

The variation of the inhomogeneity force from the model B is shown in Fig. 5 where no change is observed. The magnitude of the inhomogeneity forces is also not significantly exposed. These mean that the temperature gradient has no effect to the evolution of the inhomogeneity forces.

In order to examine the effects of crystal morphology, we consider two cases which are the magnitude of the inhomogeneity forces in the model A1 and the difference between the model A2 and the model B1. In the first case, the magnitude of the inhomogeneity forces of the model A1 are quite small for planar components compared to the model A2 and A3 which the interfacial roughness are introduced. For the second case, the model A2 has the same uniform temperature gradient and the same ratio of interfacial roughness size to the system's size as the model B1. By comparing their results, a significantly difference of the magnitude of the inhomogeneity force cannot be observed which may implies that the crystal morphology has a little effect on the evolution of the inhomogeneity force.

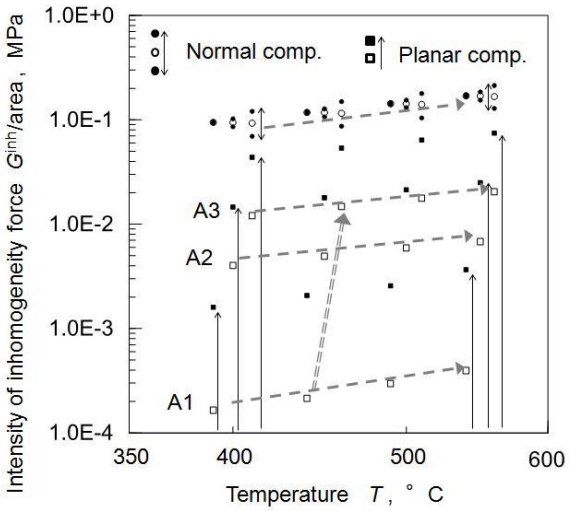

Fig. 4 Inhomogeneity forces from model A.

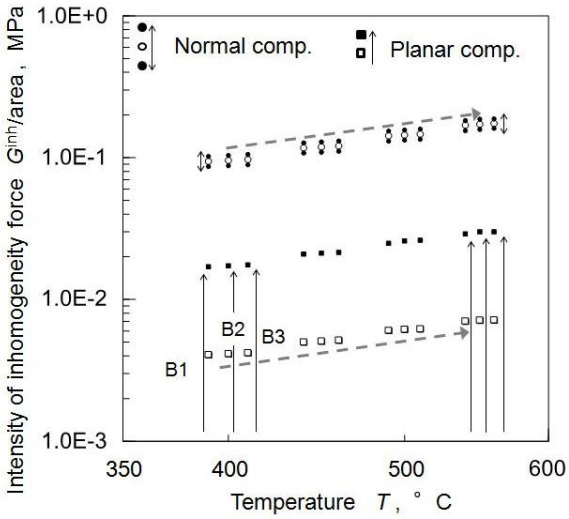

Fig. 5 Inhomogeneity forces from model B.

6. Conclusion

We briefly outlined the elastoplastic constitutive equations of materials with temperature dependence and inhomogeneity force based on the concepts of configurational mechanics. They are introduced to a model of surface coating in a quasi-crystal scale. A strain distribution of the film/substrate system is simulated by the finite element method. The result shows that crystal morphology of the substrate has an influence to the strain

distribution of the film. And by evaluation of the inhomogeneity forces at the interface of coated materials under thermal loads with two analytical models, the interfacial roughness would be a cause of activating the driving force of the debonding, while the crystal morphology and the temperature gradient have no influence.

7. Acknowledgement

The first author thanks the Ministry of Education, Culture, Sports, Science and Technology, Japan for the financial support. A part of this work was supported by the Japan Society of Promotion of Science as a Grant-in Aid for Scientific Research (No. 22560060), which is acknowledged.

8. References

[1] Bregman, A.M., and Kassir, M.K. (1974). Thermal fracture of bonded dissimilar media containing a penny-shaped crack, *Int. J. Fracture*, vol. 10(1), pp. 87 - 98.

[2] Chai, H., Babcock, C.D., and Knauss, W.G. (1981). One dimensional modelling of failure in laminated plates by delamination buckling, *Int. J. Solids Structures*, vol. 17(11), pp. 1069 - 1083.

[3] Evans, A.G., Drory, M.D., and Hu, M.S. (1988). The cracking and decohesion of thin films, *J. Mater. Res.*, vol. 3(5), pp. 1043 - 1049.

[4] Hutchinson, J.W., and Suo, Z. (1992). "Mixed mode cracking in layered materials", in *Advances in applied mechanics* (edited by Hutchinson, J.W. and Wu, T.Y.), vol. 29, pp. 63 - 191, Academic Press, New York.

[5] Hutchinson, J.W., He, M.Y., and Evans, A.G. (2000). The influence of imperfections on the nucleation and propagation of buckling driven delaminations, *J. Mech. Phys. Solids*, vol. 48(4), pp. 709 - 734.

[6] Wang, X., Su, D., Lu, G., and Wang, C. (2003). Non-linear thermal buckling for local delamination near the surface of laminated plates, *J. Reinf. Plast. Comp.*, vol. 22(5), pp. 419 - 439.

[7] Liu, C.J., Ernst, L.J., Wisse, G., Zhang, G.Q., and Vervoort, M. (2003). Thermally induced delamination buckling of a thin metal layer on a ceramic substrate, *ASME J. Electron. Packag.*, vol. 125(4), pp. 512 - 519.

[8] Maugin, G.A. (1993). Material Inhomogeneities in Elasticity, Chapman & Hall, London.

[9] Mueller, R., Kolling, S., and Gross, D. (2002). On configurational forces in the context of the finite element method, *Int. J. Numer. Meth. Engng.*, vol. 53(7), pp. 1557 – 1574.

[10] Imatani, S., Hatada, K., and Maugin, G.A. (2005). Finite element analysis of crack problems for strain gradient material model, *Phil. Magazine*, vol. 85(33-35), pp. 4245 – 4256.

[11] Kienzler, R., and Herrmann, G. (2000). Mechanics in Material Space : with Applications to Defect and Fracture Mechanics, Springer-Verlag, Germany.

[12] Eshelby, J.D. (1951). The force on an elastic singularity, *Phil. Trans. R. Soc. Lond. A*, vol. 244, pp. 87 - 112.

[13] Liu, W.K., Ong, J.S., and Uras, R.A. (1985). Finite element stabilization matrices, *Comput. Method Appl. M.*, vol. 53(1), pp. 13 - 46.

[14] Imatani, S., and Thammakornbunjut, E. (2011). Possible debonding mode of coated film

under thermal loading, *Int. J. Eng. Sci.*, doi:10.1016/j.ijengsci.2011.04.004, (in press).

[15] Spencer, A.J.M. (1971). "Theory of invariants", in *Continuum Physics* (edited by Eringen, A.C.), Academic Press, New York.

[16] Hill, R. (1950). The Mathematical Theory of Plasticity, Oxford University Press.

[17] Cherepanov, G.P. (1985). "Configurational forces in the mechanics of a solid deformable body" PMM (English transl), vol. 49(4), pp. 456 - 464.

[18] Gurtin, M.E. (1995). "The nature of configurational forces", Arch. Rational Mech. Anal., vol. 131, 67 - 100.

[19] Kienzler, R. and Herrmann, G. (1986). "Material forces in elementary beam theory", J. Appl. Mech.- T ASME, vol. 53, pp. 561 – 564.

[20] Maugin, G.A. and Trimarco, C. (1992). "Pseudomomentum and material forces in nonlinear elasticity : variational formulations and application to brittle fracture", Acta Mech., vol. 94, pp. 1 – 28.

[21] Rice, J.R. (1968). "A path independent integral and the approximate analysis of strain concentrations by notches and cracks", J. Appl. Mech. – T ASME, vol. 35, pp. 379 - 386.